ELSEVIER

Catalysis Today 35 (1997) 293–317

CATALYSIS TODAY

Sol–Gel preparation of supported metal catalysts

Richard D. Gonzalez [a,*], Tessie Lopez [b], Ricardo Gomez [b]

[a] *Department of Chemical Engineering, Tulane University, New Orleans, LA 70118, USA*
[b] *Universidad Autonoma, Metropolitana-I, P.O. Box 55-534, Mexico, D.F., Mexico*

Abstract

Variables important in the synthesis of supported metal catalysts using the sol–gel method are reviewed. Potential applications of these materials are presented with emphasis on: thermally resistant materials, catalysts with low deactivation rates, high surface area materials, catalytic membrane reactors and high surface area superacid materials. Emphasis is on synthesis conditions including the control of variables which enable the preparation of well defined pore size distributions. The reforming reactions of *n*-hexane are used as a basis for comparison between catalysts.

1. Introduction

1.1. Supported metals in catalysis. The need for new methods

Supported metal catalysts currently in use in applications such as automotive exhaust emission control, petroleum reforming and NO_x conversion are reasonably resistant to sintering at temperatures up to about 550°C. However, excursions in excess of this temperature may result in metal crystallite growth. Sintering not only results in the loss of exposed metal surface area but may also lead to changes in the catalytic properties of the supported metal. Research on the mechanism of sintering and on the stability of supported metal catalysts has been the subject of intense study during the last thirty years. An excellent review on the subject has appeared in a book edited by Stevenson et al. [1]. This review discusses both the theoretical and experimental aspects of sintering. In the case of Pt/SiO_2 catalysts, both planar [2] and porous substrates have been studied [3]. Numerous approaches have been suggested in order to stabilize supported metal catalysts in the high temperature range. Ruckenstein and Pulvermacher [4] have proposed the generation of a chemical trap on the substrate to inhibit sintering. Irregular substrates have valleys and the atoms of the substrate may generate energy wells. In a theoretical study, they suggested that a narrow distribution of particle sizes could be attained through the use of these chemical traps. Using theoretical models, Ruckenstein and Pulvermacher [5] suggest that when the size of a crystallite is matched to the diameter of the pore, surface diffusion is inhibited and crystal growth will not occur. The addition of a second oxide (BaO for example) to alumina appears to inhibit sintering [6]. It is thought that this inhibition to sintering occurs as a result of the forma-

* Corresponding author.

PII S0920-5861(96)00162-9

tion of M–O–N linkages between the supported metal and the modifying oxide. Pan and Ciprious [7] have reported that the sintering of Pt crystallites is inhibited by the presence of phosphorous on a carbon substrate. Sulfur may also delay sintering by preventing the aggregation of Pt atoms [1].

Palladium-only automotive catalysts as a possible replacement for three-way (Pt–Rh–Pd) catalysts have been the subject of considerable study [8,9]. In addition to its low cost, an all-palladium automotive catalyst has been claimed to have higher thermal stability than traditional three-way catalysts. The reason for this is that Pd is very stable in an oxidizing atmosphere. In particular, the formation of PdO was observed to occur readily between 365 and 370°C in flowing oxygen [10,11]. The dissociation temperature of PdO is about 800°C [12–15]. Pt and Rh, on the other hand, are more stable in a reducing atmosphere [16,17]. Lean burn engines are being developed by automakers in the hope of improving fuel efficiencies. Air-to-fuel ratios can be raised from a current stoichiometric ratio of 14.65 to 18 or even to 21 [18]. Because of the higher thermal stability of Pd-only catalysts in an oxygen rich atmosphere, the use of palladium-only catalysts allows the converter to be placed closer to the exhaust manifold. This results in a faster activation of the catalyst and a reduction in emissions.

The thermal stability of supported Pd catalysts has received considerable attention during the last three decades. Sintering of Pd/Al_2O_3 in hydrogen at 650°C for 1 h results in a 50% decrease in metal dispersion [19,20]. The range of metal particle sizes of Pd/SiO_2 was observed to increase by 50% following treatment in H_2 at 600°C [21,22]. The formation, high stability, and decomposition (redispersion) of palladium oxide (PdO) on silica or alumina supports has been studied by several researchers [10–15,23–25]. The formation and splitting of palladium hydrides (β-Pd–H) on silica or alumina supports has also been reported [23,26,27]. A mechanism for the sintering of Pd supported on alumina has been proposed by Chen and Ruckenstein [28]. This mechanism includes:

1. Crystallite migration and coalescence via surface diffusion;
2. Duct ripening; and
3. Ostwald ripening

The synthesis of thermally stable sulfate promoted Pt/ZrO_2 catalysts for possible application in such reactions as: skeletal isomerization [29], the ring-opening isomerization of cyclopropane [30], the polymerization of ethers [31], and the acetylation of alcohol with acetic acid [32] has attracted considerable attention. The characteristic structures of these sulfate ion-promoted metal oxides is as follows [33]:

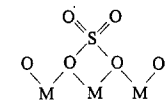

In particular, the superacid properties of SO_4^{-2}/ZrO_2 have made it extremely attractive in commercial applications related to the upgrading of petroleum feeds which have low octane ratings.

Unfortunately, a disadvantage in the use of sulfate ion-promoted zirconia catalysts is deactivation due to coke formation and the decline in the concentration of strong Bronstead acid sites. For this reason, the catalyst lifetime is not sufficient for industrial use. Baba et al. [34] have reported that the addition of Pt to SO_4^{-2}/ZrO_2 improves both its catalytic activity and lifetime in the skeletal isomerization of pentane. Presumably the addition of Pt increases the rate of methane formation and, therefore decreases the rate of carbon formation. On the other hand, the addition of too much Pt may result in a change in the surface chemistry. In particular, care must be taken to insure that one is simply not synthesizing a bifunctional reforming catalyst in which dehydrogenation to form an olefin followed by protonation to form a carbonium ion is occurring over the metal. This carbonium ion may then migrate to the acid sites on ZrO_2 and

isomerize. The chemistry is, therefore, quite different from what apparently occurs on the superacid sites of zirconia in the absence of Pt. A second problem associated with the addition of Pt is that it sinters rapidly as a result of activation in air at 600°C. For this reason, methods aimed at synthesizing stabilized platinized zirconia catalysts would be beneficial.

Membranes made from inorganic materials such as metals, ceramics and inorganic polymers have been developed for gas and liquid separations. By separating products from reactants in a catalytic membrane rather than downstream of the reaction should result in an increase in the equilibrium yield of the reaction [35]. By taking advantage of the narrow pore size distribution of supported metal catalysts prepared by the sol–gel method, it is possible to combine the separative and catalytic properties of membrane reactors. For example, consider the dehydrogenation of butane which takes place over a supported Pt catalyst. A thermally stable supported Pd/SiO_2 catalyst can be prepared by the sol–gel method described by Zou and Gonzalez [36]. To produce the supported membrane, a preformed α-Al_2O_3 ceramic support is interfaced with Pt/SiO_2 on the feed side and Pd/SiO_2 on the product side of the reactor. The slip casting method can be used to prepare the membrane reactor [37].

1.2. The advantages of the sol–gel approach over traditional methods of preparation

Sol–gel processing provides a new approach to the preparation of supported metal catalysts. A well-defined pore size distribution can be obtained using this approach. The potential advantages of sol–gel processing include: purity, homogeneity, and controlled porosity combined with the ability to form large surface area materials at low temperatures. The use of high-surface area aerogels for catalyst supports has been described in detail by Teichner [38]. Important variables which must be considered in the synthesis of supported metals by the sol–gel method include: pH, reactant stoichiometries, gelation temperature, metal loading, solvent removal and pretreatment condition. The purpose of this review is to consider how these variables come into play during synthesis and to review the influence that these variables have on the chemistry of the sol–gel synthesis.

2. One step preparation of supported metal catalysts

2.1. The preparation of supported metal xerogels and aerogels

Several methods have been used to prepare supported metal catalysts, the most import being: (i) Precipitation or coprecipitation. In this method, one or more soluble salts which contain the metal of interest are neutralized through the addition of a base (usually ammonia) to form a precipitate or coprecipitate of the corresponding metal oxide gels [39]. (ii) Impregnation, in which the support (silica, alumina, magnesia, titania, zirconia, etc.) is contacted with a solution which contains the metal to be deposited on the support. A suspension is initially formed. This suspension is heated under continuous mixing in order to evaporate the solvent and to disperse the metal on the support [40–42]. (iii) Ion-exchange, which consists in exchanging either hydroxyl groups or protons from the support with cationic or anionic species in solution. In this method, it is important to adjust the pH in order to maximize the electronic interaction between the support and the metal precursor. A knowledge of the isoelectric point is essential if meaningful dispersions are to be obtained [43,44]. (iv) Sol–gel processing in which metalorganic precursors are mixed with metal precursors to form a homogeneous solution. The metalorganic precursor is hydrolyzed through the addition of water while carefully controlling the pH and the reaction temperature. As hydrolysis and polymerization occur, colloidal particles or micelles with an approximate diameter of 10 nm are

formed. These particles continue to increase in size until a metal oxide gel is formed [45–52]. The solvent can be eliminated by heat treatment in air to form a xerogel or in an autoclave under supercritical conditions to form an aerogel. The uniqueness of the support method is that one starts with the molecular precursor of the support material and then goes all the way to the final catalyst. A greater degree of control over the catalyst preparation can be achieved in comparison to traditional methods of preparation [53]. One can "tailor make" catalysts to fit particular applications by using this method. Advantages include: (i) superior homogeneity and purity; (ii) better microstructural control of metallic particles; (iii) higher BET surface area; (iv) improved thermal stability of the supported metals, (v) well-defined pore size distributions; (vi) the ease with which additional elements can be added; (vii) inorganic chain-structures can be generated in solution; and (viii) a finer degree of control over the hydroxylation of the support can be obtained.

The molecular compounds which are formed as a result of the copolymerization of the organic and inorganic precursors using the sol–gel synthesis approach, have unusual physical and chemical properties. They form stable solid structures at low reaction temperature with unusually high surface areas. Particle sizes are in the nano size range and they have additional physical and chemical properties which make them useful as either catalysts or catalyst supports [54–57].

The synthesis of xerogels and aerogels occurs in two distinct steps. During the initial stage, usually referred to as "pregelation", the reactants (alcoxides and metal precursors) hydrolyze and condense to form a gel. The hydrolysis occurs when water is added to the alcoxide which is usually dissolved in alcohol or some other appropriate solvent. Intermediates obtained as a result of this reaction include: oligomers of the acid which corresponds to the alcoxide used and ether oligomers which are finally transformed into gels and contain large amounts of water in their structure. In addition to these oligomers, a nonhomogeneous crystalline microstructure encapsulated within the initial amorphous solid is also formed (gel). In the condensation or polymerization reactions, alcoxi groups (M–OR) react with hydroxyl groups (M–OH) formed during the hydrolysis to form metaloxanes (M–O–M). During this step the primary structure and the properties of the gel are determined. The reactions which take place are as given in Scheme 1.

These reactions occur simultaneously and usually do not go to completion. A schematic which shows the gelation of a silicon alcoxide is shown in Fig. 1. It is important to note that the conditions under which the condensation reactions occur are important in determining the nature of the final product as either a gel or a precipitate. Condensation/hydrolysis can take place by two different mechanisms which depend on the coordination of the central metal atom. When the preferred coordination is satisfied, hydrolysis occurs by nucleophilic substitution (S_n) as in Scheme 2.

When the preferred coordination cannot be satisfied, hydrolysis can occur by nucleophilic addition (A_n), as in Scheme 3.

These mechanisms require that the coordination of oxygen be increased from 2 to 3, as in titania for example. The creation of the addi-

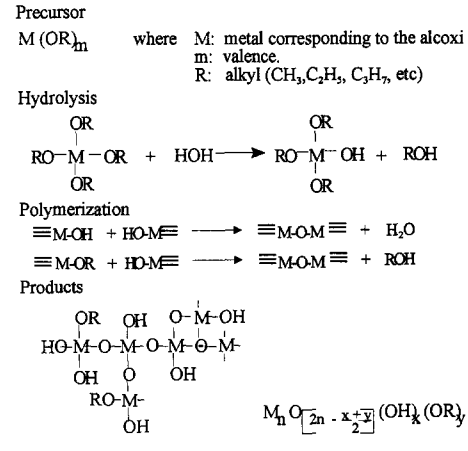

Scheme 1.

tional bond involves a lone pair of electrons on the oxygen, and the bond which is formed may be equivalent to the other two bonds [58,59].

During the condensation stage a large number of hydroxyl groups can be formed. These hydroxyl groups may either be bridging groups

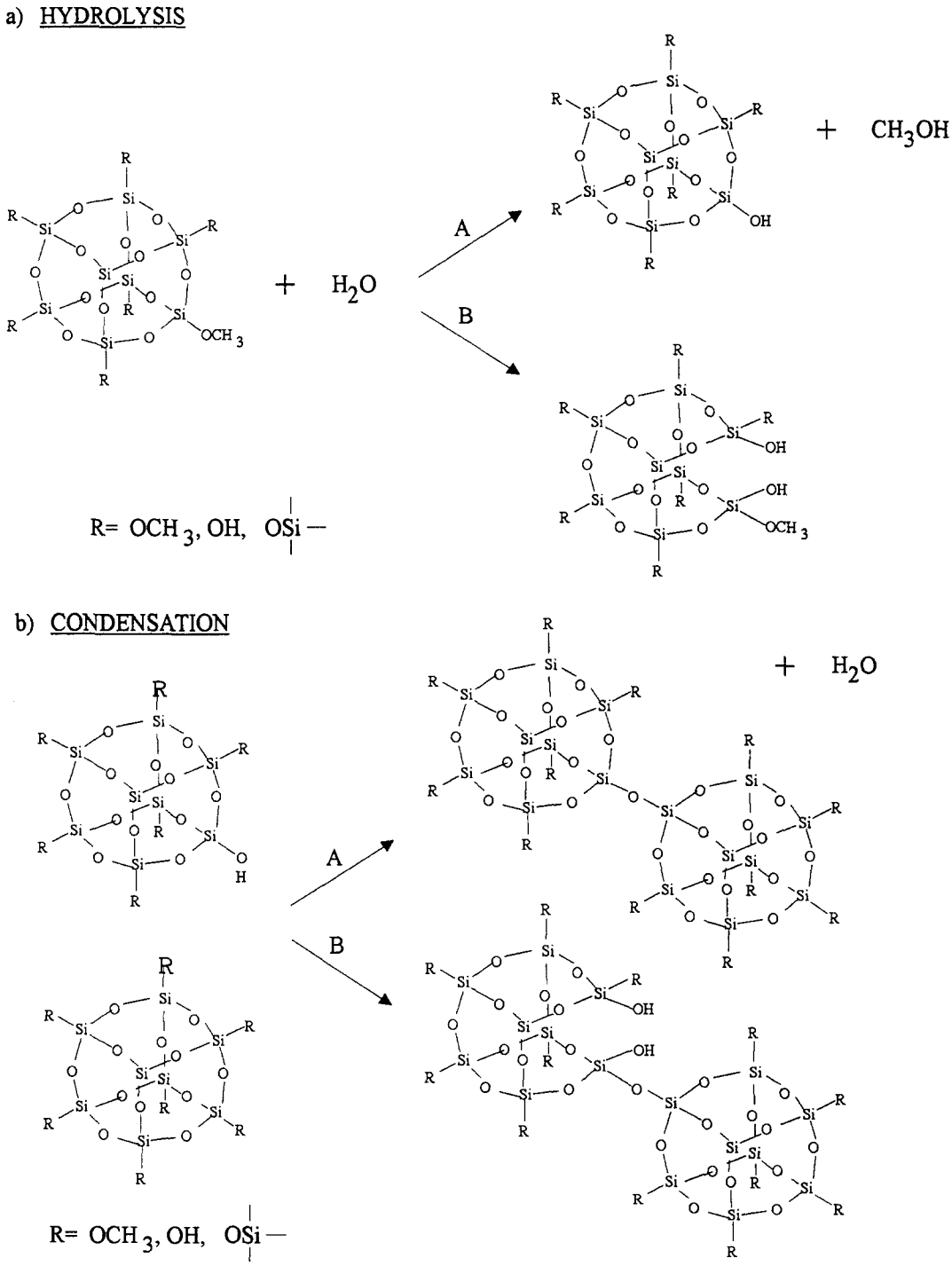

Fig. 1. (a) Hydrolysis reaction, (b) condensation reaction.

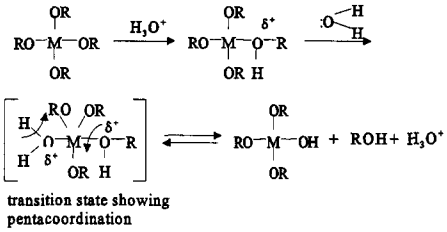

Scheme 2.

between metal centers or simple OH ligand [60–63] (Scheme 4).

The second stage in the sol–gel synthesis is referred to as the "postgelation" step. Changes which occur during the drying and calcination of the gel include: the desorption of water, the evaporation of the solvent, the desorption of organic residues, dehydroxylation reactions and structural changes. The evaporation of the solvent during drying leads to the formation of strong capillary forces. These capillary forces arise from the difference between solid–vapor and solid–liquid interfacial energies. The huge interfacial area of the gel (300–1000 m^2/g) can result in capillary pressures as large as 100 MPa [63]. Because it is possible to develop large pressure gradients within the gel structure, the network is compressed to a greater extent at the exterior surface. This differential strain results in cracking. Solvent removal under supercritical drying conditions (243°C) and 63 atm for ethanol results in the elimination of the liquid–vapor interface and a preservation of the gel microstructure (aerogel). Milder evaporation conditions can be achieved using CO_2 rather than ethanol. A comparison in the microstructure of the xerogel and the aerogel prepared under identical conditions shows that the adsorption of N_2

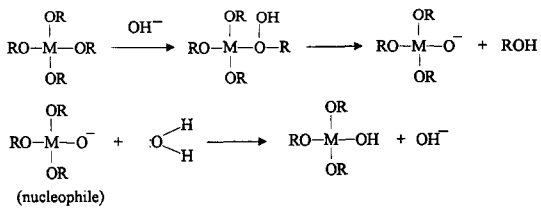

Scheme 3.

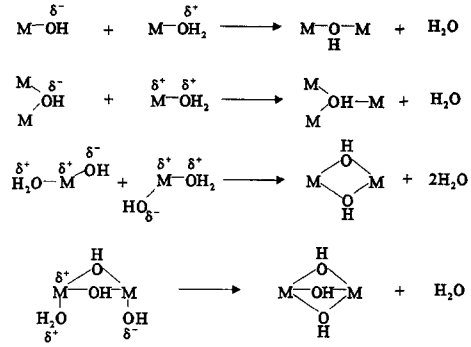

Scheme 4.

is quite different [64]. For the xerogel, the adsorption of H_2 is distinctly Langmuir while N_2 adsorption on the aerogel follows a BET type II adsorption isotherm [44,50]. Pore volumes for the aerogel and the xerogel differ by an order of magnitude. Densification of the xerogel following thermal treatment is shown in Figs. 2 and 3.

Because there is considerable difference in the sol–gel chemistry between silica and other supports such as alumina [50,64], it is important to understand the effect of variables such as: H_2O/alcoxide ratios, reaction pH, the influence of the solvent, time, temperature of reaction, the effect of different alkyl groups, and the metallic precursor used.

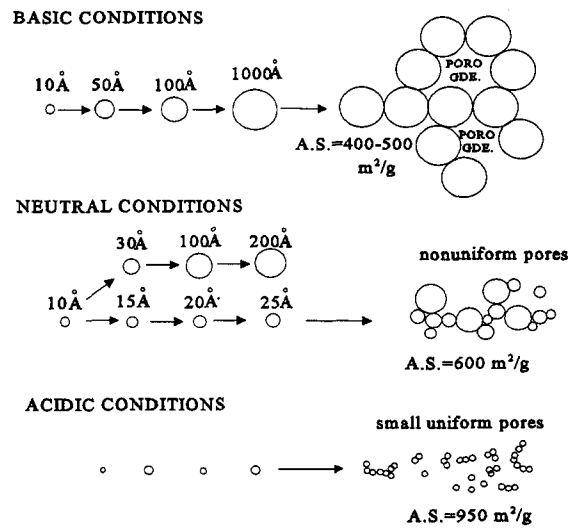

Fig. 2. The formation of a gel from a colloidal solution.

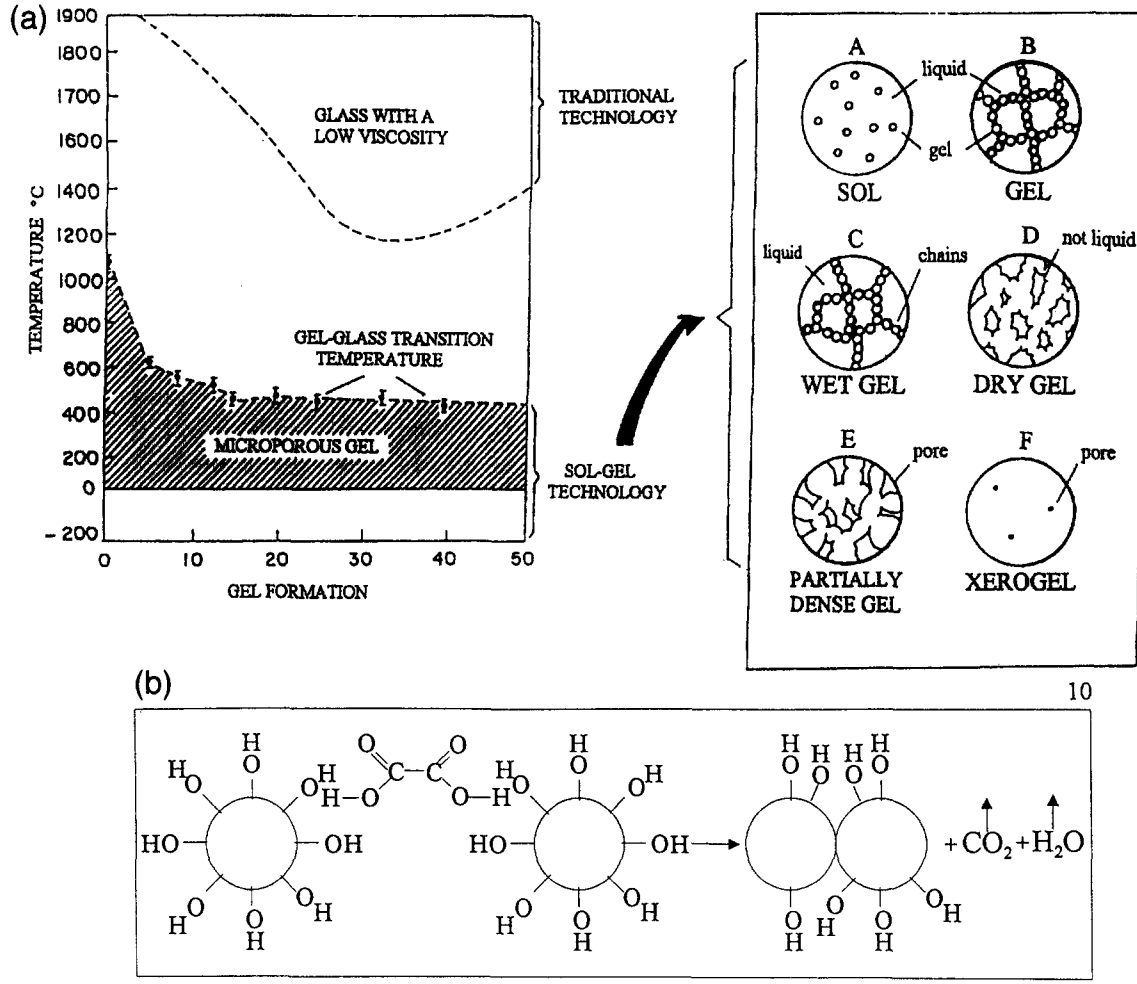

Fig. 3. (a) Post gelation stage, (b) densification.

2.1.1. Effect of the water to alcoxide ratios

A large number of studies have been performed in an effort to understand the effect of water on the properties of the gel [63,65–68]. When non-stoichiometric amounts of water were added to silicon alcoxides such as tetraethoxysilane (TEOS) or tetramethoxysilane (TMOS), an analysis of the reaction products showed that the extent of polymerization was largely dependent on the number of moles of water which was added. In the case of substoichiometric quantities of water, the hydrolysis of the alcoxide was not complete, and linear oligomers, as opposed to branched ones, were obtained. When the H_2O/alcoxide ratio was in excess of that required for stoichiometry, hydrolysis was observed to approach completion. This increase in the extent of the hydrolysis was observed to lead to highly branched polymeric products, as given in Scheme 5 and Scheme 6.

When the H_2O/alcoxide ratio is increased, the time required for the formation of the gel is also observed to increase. This same result is also obtained when the pH is decreased [44].

Yamane et al. [67], Gonzalez et al., [44,50] and Lopez et al. [69,70] have reported the effect of the H_2O/alcoxide ratio on the physical properties of a series of oxides and mixed oxides prepared by the sol–gel method. These studies are summarized in Table 1. It is important to

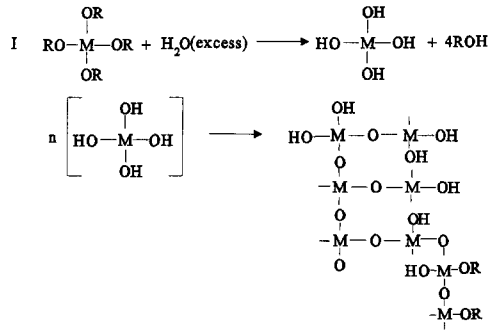

Scheme 5.

stress that BET surface areas and pore size distributions were obtained following calcination at 650°C.

In the case of silica an increase in the H_2O/alcoxide ratio results in an increase in the BET surface area with a concomitant decrease in the pore diameter [67,44]. The increase in BET surface area and the decrease in the pore diameter is, in all likelihood, related to the increase in cross linking as a result of the increase in the extent of the hydrolysis at the high H_2O/alcoxide ratios. In the case of the

Table 1
The effects of the H_2O/alkoxide ratio on the physical properties of several xerogels

Catalyst	H_2O/ alkoxide	BET (m^2/g)	Pore diameter (nm)	Ref.
SiO_2	4.2	734	–	[67]
SiO_2	5.1	740	–	[67]
SiO_2	12.4	806	–	[67]
Al_2O_3	3.0	469	9	[50]
Al_2O_3	15.0	260	15	[121]
SiO_2–Al_2O_3	0.27	783	–	[69]
SiO_2–Al_2O_3	0.55	621	–	[69]
SiO_2–Al_2O_3	1.36	501	–	[69]
Pt/(5%SiO_2–95%Al_2O_3)	3.0	529	8	[50]
Pt/(10%SiO_2–90%Al_2O_3)	3.0	512	4	[50]
Pt/SiO_2	3.0	474	20	[44]
Pt/SiO_2	6.0	495	15	[44]
Pt/SiO_2	10.0	632	16	[44]
Pt/SiO_2	15.0	721	8	[44]
Pt/SiO_2	20.0	784	4	[44]
Pt/Al_2O_3	1.5	222	5	[50]
Pt/Al_2O_3	3.0	490	9	[50]
Pt/Al_2O_3	9.0	363	15	[50]

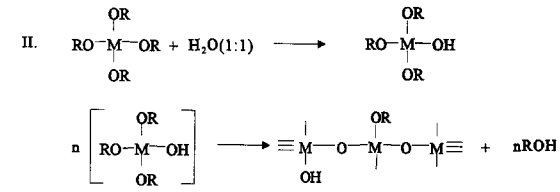

Scheme 6.

alumina gels, the relationship between BET surface areas and the H_2O/alcoxide ratio appears to be more poorly defined. Substoichiometric H_2O/alcoxide ratios lead to narrower pore size distributions. An increase in the H_2O/alcoxide ratio clearly leads to an increase in the pore diameter [50]. The surface area appears to go through a maximum when the H_2O/alcoxide ratio is close to that corresponding to stoichiometry. When aluminum *t*-butoxide (ATB) is used as the precursor, this stoichiometric ratio is 3. The addition of silica to alumina to form a mixed oxide accomplishes two things: (1) a decrease in the average pore diameter occurs and, (2) the amorphous phase of alumina is stabilized [50].

Changes in surface area and gelation time as a function of the H_2O/TEOS ratio for silica at a constant pH of 1.3 and a reaction temperature of 50°C are shown in Fig. 4 [44]. A substantial increase in both the surface area and the time required for gel formation to occur was ob-

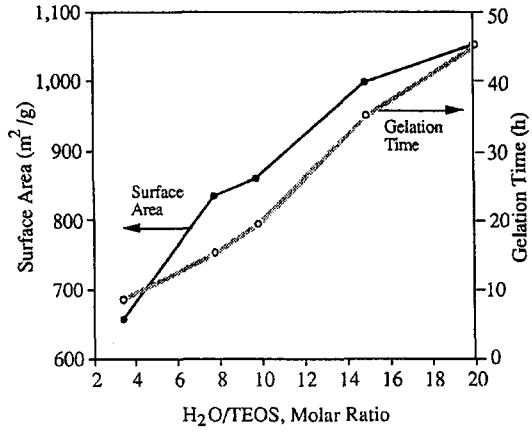

Fig. 4. Changes in surface area and gelation time as a function of the H_2O/TEOS ratio at a constant pH of 1.3 and a gelation temperature of 50°C [12].

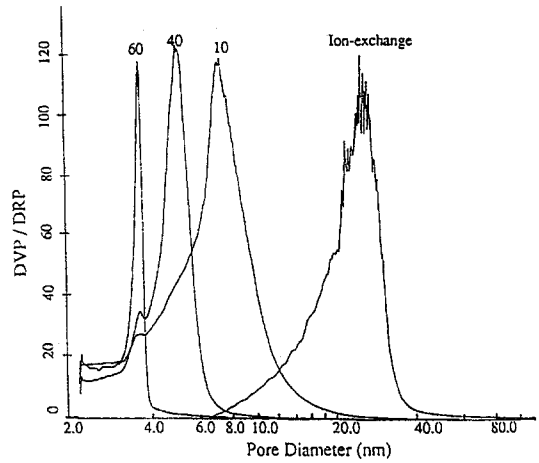

Fig. 5. The pore size distribution of Pt/SiO_2 prepared using $Pt(AcAc)_2$ as a function of H_2O/TEOS ratio with the same designed metal loading (1 wt%) following pretreatment in O_2 at 400°C for 1 h, and H_2 at 400°C for 3 h [12].

served when the H_2O/TEOS ratio was increased from 2 to about 20. The pore size distribution for a series of Pt/SiO_2 catalysts (2% metal loading) as a function of the H_2O/TEOS ratio with all of the other preparative variables kept constant are shown in Fig. 5 [44]. It should be noted that the pore diameter decreases and the pore size distribution narrows sharply as the H_2O/alcoxide ratio is increased.

A word should be mentioned concerning the effect of prehydrolysis on the structural properties of the mixed metal oxides reported in Table 1. This is because different metallic alcoxides display different chemical reactivity towards nucleophilic reactions depending primarily on two parameters, namely, the electrophilic character of the alcoxide and their degree of unsaturation [71]. Silicon alcoxides are much less reactive in comparison to the corresponding transition metals, rare earths and aluminium alcoxides [71]. The effects of prehydrolysis on the physical properties of a 1 wt% Pt/(95% alumina–5% silica) are shown in Table 2 [50].

Table 2
Effects of prehydrolysis for pretreated 1 wt% Pt (95% alumina–5% silica) mixed metal oxide samples

Prehydrolysis	BET (m^2/g)	Pore volume (cm^3/g)	Average diameter (nm)	Dispersion (%)
No	529	1.641	8	61
Yes	538	1.958	7	89

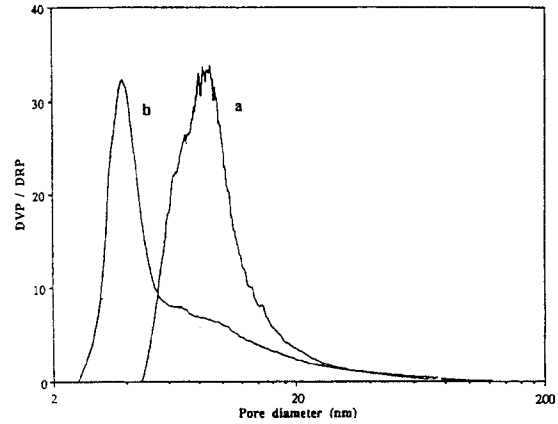

Fig. 6. Effect of mixing the alumina support with silica for pretreated 1.0 wt% Pt xerogel samples supported on the following supports: (a) 100% alumina and (b) 90% alumina–10% silica.

The most significant difference between the two samples is the increase in dispersion obtained when the TMOS (tetra methoxy silane) is prehydrolyzed.

The effect of forming the mixed oxide on the pore size distribution is shown in Fig. 6 [50]. The addition of 10% silica to alumina not only results in a catalyst with higher thermal stability but also a substantial decrease in the pore size distribution from 9 nm to 4 nm.

2.1.2. The effect of pH

The synthesis of solid catalysts using sol–gel processing may be performed under acid conditions (pH 1.5–6), basic conditions (pH 8–11) or neutral conditions (pH 7). Different catalysts can be used to perform the hydrolysis reactions. Under acid conditions, strong acids such as HCl, H_2SO_4, HF, etc. may be used as catalysts. Weak acids or weak bases such as acetic, oxalic, formic or ammonia may also be used. It should be remembered that a pH in excess of 11 will lead to the dissolution of silica. Boonstra [72] reported that under strongly acidic conditions, hydrolysis occurred very rapidly and that gel formation times were increased substan-

tially. Andrianov [73] proposes that hydrolysis reactions under acidic conditions involves the displacement of an OR group by a nucleophilic SN_2 type substitution reaction. Under acidic conditions, it is likely that an alcoxide group is protonated in a rapid first step. Electron density is withdrawn from silicon, making it more electrophilic and thus more susceptible to attack by water. The water molecule attacks from the rear and acquires a partial positive charge. The positive charge on the protonated alcoxide is reduced. This results in a transition state in which the removal of the alcohol group is facilitated (Scheme 7).

The anion corresponding to the acid attacks the central metal atom increasing its coordination. The hydrolysis takes place through the M–X bond of the transition state species. When hydrolysis occurs under basic conditions, the reaction follows a nucleophilic bimolecular substitution pathway. Hydrolysis is slower and the polymerization is catalyzed by the base. Under these conditions, gelation times are considerably slower. Aelion [74] obtained reaction rate constants when the reaction was performed under acid conditions. Both acid concentration and acid strength are important variables in determining hydrolysis reaction rates. When HCl was used to catalyze the reaction, Aelion [74] observed a first order dependence in (HCl). Both alcohol and H_2O are reaction products, and therefore their concentration never reaches zero [75] following the completion of the reaction. Temperature and solvent appear to be of less significance. Strong acids behave in a similar fashion, whereas weaker acids require longer reaction times to achieve the same extent of reaction.

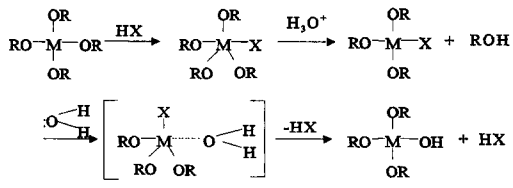

Scheme 7.

When the reaction was performed under basic conditions, the order of reaction was determined by a comparison of the times required to achieve a specific extent of hydrolysis. When dilute concentrations of a strong base are used, the reaction was observed to follow a first order rate dependence. When weaker bases such as pyridine or ammonia were used, the reaction rate only increases when very high concentrations of base were used. Under basic conditions it is likely that hydrolysis occurs via a nucleophilic attack of a hydroxyl group on the metal. An alcoxide ion is displaced and this displacement may be aided by hydrogen bonding of the alcoxide anion to the solvent.

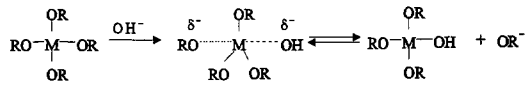

The metal acquires a formal negative charge in the transition state. Electron withdrawing substitutes such as –OH or –OM should help stabilize the negative charge on the metal, causing the hydrolysis rate to increase with the extent of OH substitution, whereas substitutes that are electron donors should decrease reaction rates.

The effects of a variety of catalysts on the overall hydrolysis and condensation rates of TEOS have been summarized by Pope et al. [76]. These studies point to the importance of hydrogen and hydroxyl ions on the time required for gelation to be complete. However, the conjugate ions of the base and the acid also play an important role.

The reaction pH is very important in determining the final properties of the material which is synthesized. Under basic conditions, the particles which are initially formed have a diameter of approximately 1 nm (see Fig. 3). These particles increase in size during the synthesis. The resultant gel tends to be mesoporous or macroporous. When the reaction is performed at a pH of 7, the particles in the sol vary between

2.5 and 20 nm. For this reason, the resultant gel has a non-uniform pore size distribution. Under acid conditions the particles in both the sol and the gel are very uniform. They vary in size between 0.5 and 3.0 nm and in general have very high porosities. Under highly acidic conditions, micropores predominate (< 2 nm) and N_2 adsorption is best described using the Langmuir equation rather than the BET equation [44]. These results are shown in Fig. 7.

Surface areas and average pore size distributions of silica xerogel as a function of pH are shown in Fig. 7. A substantial decrease in the surface area together with a concomitant increase in pore size distribution was observed with increasing pH. A sharp decline in surface area occurs at a pH of approximately 8.5. It is also important to note that the pore volume

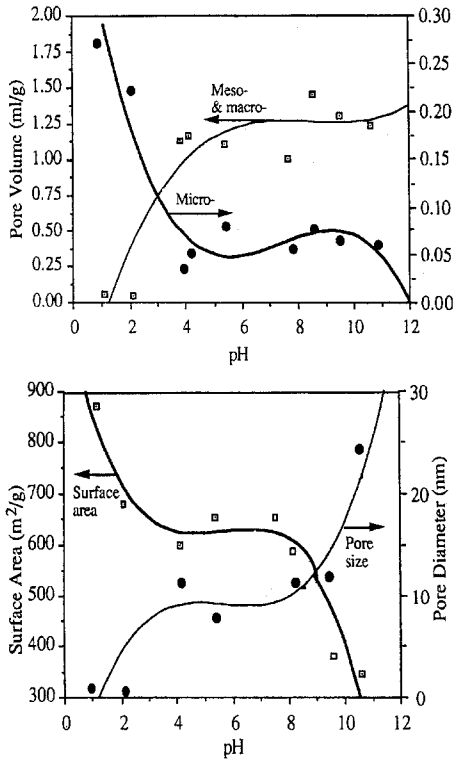

Fig. 7. (top) Changes in micro-, meso- and macro-pore volume as a function of pH at a constant H_2O/TEOS ratio of 10, and a gelation temperature of 50°C [12]. (bottom) Changes in surface area and pore size as a function of pH at a constant H_2O/TEOS ratio of 10, and a gelation temperature of 50°C [12].

Table 3
The effect of pH on the BET surface area and particle size distribution of several catalysts prepared by the sol–gel method

Catalyst	pH	BET surface area (m^2/g)	Av. pore diameter (nm)	Ref.
Al_2O_3	3	270		[122]
Al_2O_3	6	322		[122]
Al_2O_3	9	350		[122]
Al_2O_3	10.3	425		[50]
MgO	3	44		[78]
MgO	5	35		[78]
MgO	9	67		[78]
Pt/SiO_2	3	540	4	[83]
Pt/SiO_2	5	632	44	[83]
Pt/SiO_2	9	1134	2	[83]
Pd/SiO_2	3	457	2	[40]
Pd/SiO_2	9	188	70	[95]
Ru/SiO_2	3	450	10	[85]
Ru/SiO_2	9	672	4	[85]
Pt/MgO	3	16		[79]
Pt/MgO	9	26		[79]

corresponding to meso (2–50 nm) and macro (> 50 nm) pores increase at the expense of micropores (< 2.0 nm) [77] with increasing pH. In general, pore volumes associated with meso and macropores are about one order of magnitude larger than micropore volumes.

The effect of pH on surface area and average pore diameters of a number of solids prepared using alcoxide precursors is summarized in Table 3. The properties shown in Table 3 were obtained following calcination in air at relative high temperatures. Balakrishnan and Gonzalez [50], for example, report a surface area of 900 m^2/g of alumina prepared using ATB (aluminum trisecbutoxide) at a pH of 10.3. Following calcination at 600°C, the surface area was observed to decrease to 425 m^2/g. This sharp drop in surface area is due to a phase transformation from amorphous to γ-alumina. This large surface area drop following calcination is not observed for silica. In fact, the addition of approximately 10% SiO_2 to alumina to form a mixed oxide, results in the thermal stabilization of alumina by approximately 150°C [50].

The synthesis of magnesia using magnesium

ethoxide as a precursor results in surface areas that are rather low. However, they are considerably larger than those corresponding to commercial magnesia. The largest surface areas of magnesia correspond to those obtained under basic conditions [78]. In the case of Pt/MgO the surface area was observed to go through a maximum at a pH of 7 [79]. These results have been explained by invoking a structural relaxation of the magnesia framework [80–82]. Preparation of these magnesia catalysts was performed under acid conditions using HCl and CH_3COOH and under basic condition using NH_4OH.

The data in Table 3 should be interpreted with some caution as other variables may override the effect of pH. Some generalizations can be made: For silica, everything else being held constant, the surface area falls with increasing pH [44]. For alumina [50], the surface area is roughly constant as a function of pH. Following calcination at 600°C, a phase transition from amorphous to γ-alumina occurs resulting in a BET surface area which is roughly constant (~ 450 m^2/g). The occurrences of local maxima as a function of pH appear to occur for Pt/MgO and also for Pt/SiO_2 [44]. The effect of the H_2O/alcoxide ratio may easily override pH effects. Differences in the physical properties of silica and alumina may be due to the different rates at which alcoxides undergo hydrolysis. Alumina hydrolyzes much more rapidly than silica [50].

2.1.3. *The effect of the metal precursor and the method of preparation on physical properties*

A variety of metal precursors and synthetic techniques have been used to disperse metals on the surface of xerogels and aerogels. Zou and Gonzalez [44] prepared a series of Pt/SiO_2 and Pt/Al_2O_3 [50] xerogels and aerogels. The difference in surface properties of Pt/SiO_2 catalysts are compared in Table 4. The preparations differ only in the procedure used to evaporate the solvent.

The xerogel was observed to be microporous and N_2 absorption conformed to a Langmuir plot (Type I). The aerogel, on the other hand, was macroporous and conformed to a BET Type II isotherm. The pore volumes differ by about an order of magnitude.

Table 4
A comparison between xerogel and aerogel silica supports prepared at a pH of 1.3 and a H_2O/TEOS ratio of 1.5

Sample	Surface area (m^2/g)	Pore diameter (nm)	Ref.
Xerogel	1003	< 2	[44]
Aerogel	992	18	[44]

Lopez et al. [83] used several different preparative methods to synthesize a series of Pt/SiO_2 catalysts (Fig. 8). In the first method, the alcoxide (TEOS), the solvent, the water and the metal salt were mixed to form the reactant mixture. In the second method, TEOS was added drop by drop during the final step in order to complete the reaction. In the final method, the resultant xerogel was impregnated with H_2PtCl_6 by a traditional impregnation technique. Armor et al. [84], on the other hand, added a solution of ATB to a second solution consisting of palladium acetate dissolved in warm acetone. The desired amount of H_2O was added during the final step of the synthesis.

The physical properties of the resulting gels are shown in Table 5.

Zou and Gonzalez [44] used three different metal precursors in order to form a comparison base for the preparation of Pt/SiO_2 catalysts by the sol–gel method. These catalysts were prepared using identical metal loadings. The actual metal loadings obtained by ICP were similar for all three catalysts (Table 5, Ref. [44]). When $H_2PtCl_6 \cdot xH_2O$ was used (pH 1.4), at a H_2O/TEOS ratio of 6, a microporous catalyst which had a rather high surface area (653 m^2/g) and a small pore volume (0.28 ml/g) was obtained. Dispersions as measured by both H_2 chemisorption and TEM were rather low. When $Pt(NH_3)_4(NO_3)_2$ was used as the metal precursor at a H_2O/TEOS ratio of 6 (pH 4), the

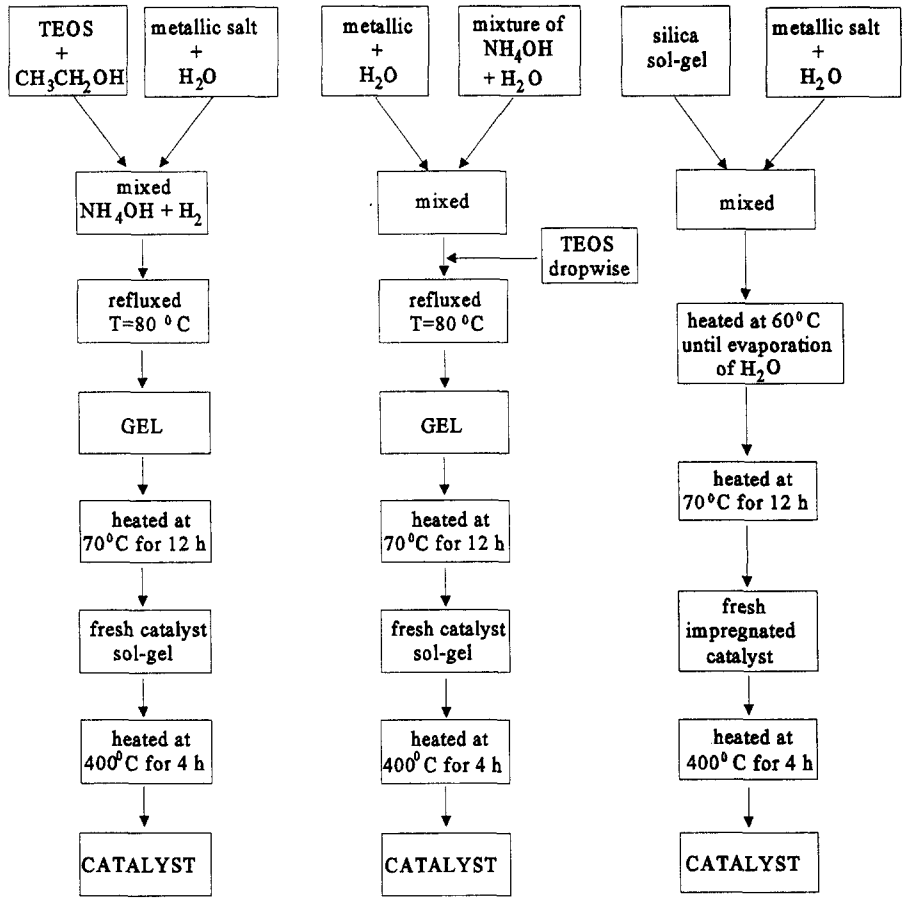

Fig. 8. Different preparative methods to synthesize a series of Pt/SiO_2 catalysts: (a) TEOS, solvent, water and metal salt in one reactant mixture, (b) TEOS added dropwise to reactant mixture, and (c) traditional impregnation with H_2PtCl_6 [83].

Table 5
The effect of different metal precursors and preparation method on the physical and chemical properties of selected xerogels

Catalyst	Metal precursor	Method	BET area (m^2/g)	Pore diameter (nm)	Dispersion (%)	Ref.
Pt/SiO_2	$H_2PtCl_6 \cdot 6H_2O$	dropwise sol–gel	653	< 2	18	[44]
Pt/SiO_2	$Pt(NH_3)_4(NO_3)_2$	dropwise sol–gel	480	4	74	[44]
Pt/SiO_2	$Pt(C_5H_7O_2)_2$	dropwise sol–gel	632	16	48	[44]
Pt/SiO_2	$H_2PtCl_6 \cdot 6H_2O$	sol–gel	680	15	–	[83]
Pt/SiO_2	$H_2PtCl_6 \cdot 6H_2O$	dropwise sol–gel	1134	< 2	–	[83]
Pt/SiO_2	$H_2PtCl_6 \cdot 6H_2O$	impregnated	91	–	–	[83]
Pt/SiO_2	$Pt(NH_3)_2Cl_2$	dropwise sol–gel	589	–	–	[70]
Pt/Al_2O_3	$H_2PtCl_6 \cdot 6H_2O$	sol–gel	490	9	74	[50]
Pt/Al_2O_3	$Pt(C_5H_7O_2)_2$	sol–gel	447	9	33	[50]
Pd/SiO_2	$Pt(C_5H_7O_2)_2$	sol–gel	722	5.5	35	[36]
Pd/SiO_2	$PdCl_2 \cdot 2H_2O$	sol–gel	634	–	–	[54]
Pd/SiO_2	$PdCl_2 \cdot 2H_2O$	impregnated	372	–	–	[54]
Pd/SiO_2	$Pd(NH_3)_2Cl_2$	dropwise sol–gel	537	2	13	[123]
Ru/SiO_2	$RuCl_3 \cdot 3H_2O$	sol–gel	672	2	70	[85]
Ru/SiO_2	$RuCl_3 \cdot 3H_2O$	impregnated	165	–	–	[85]
Pt/TiO_2	$H_2PtCl_6 \cdot 6H_2O$	dropwise sol–gel	80	8	–	[124]
Pt/TiO_2	$H_2PtCl_6 \cdot 6H_2O$	impregnated	50	30	–	[124]

resulting BET surface area was 480 m^2/g and the average pore diameter was 4 nm. This places it in the mesoporous region. Dispersions were approximately 80%. The sample prepared using $Pt(AcAc)_2$ at a H_2O/TEOS ratio of 10 resulted in a high surface area material (632 m^2/g) and moderate dispersions ($\sim$ 50%). These results were rationalized on the basis of zeta potential measurements. The isoelectric point for SiO_2 was measured and found to correspond to a pH of 2. For this reason cationic precursors at a pH of 4 would be expected to give high dispersions while anionic precursors at a pH of 1.5 should give low metal dispersions. Because $Pt(AcAc)_2$ does not have a formal charge, moderate dispersions are expected. The data confirms this hypothesis.

Attempts to impregnate xerogels and aerogels with the appropriate metal precursor using traditional methods were rather unsuccessful [44,50,83]. Evidently, the impregnating solution does not penetrate the support structure to give highly dispersed metal catalysts. Lopez et al. [83] report a large decrease in surface area to 91 m^2/g for silica following attempts to impregnate a xerogel with $H_2PtCl_6 \cdot 6H_2O$. Zou and Gonzalez [44] observed a more moderate decrease in surface area ($\sim$ 20%) following impregnation.

2.1.4. Properties of alcoxide precursors

Alcoxides are members of a family of compounds usually referred to as metalorganics. These compounds have an alkyl group which is bonded to a central metal atom through an oxygen atom [86–91]. Organometallic compounds are defined as those which contain a metal–carbon bond. According to this definition, alcoxides are not organometallics. The properties of alcoxides are, in a large measure, determined by the central metal atom and the alkyl groups bound to it through the oxygen atoms. The metal–oxygen bond is approximately 100% ionic due to the large difference in electronegativity between the central metal atom and the oxygen atom [92,93].

The three most important physical properties are:

2.1.5. Degree of oligomerization or polymerization

The formation of oligomers occurs as a result of the expansion of the sphere of coordination of the central metal atom through the formation of intermolecular bonds to neighboring alcoxide groups. Oligomerization occurs as a result of the donation of an electron pair from an oxygen atom to a vacant metal orbital.

The degree of association will depend on the central metal atom and the relative size of the alkyl group. In certain cases, it has been determined that the degree of oligomerization is dependent on the solvent and on the concentration of solute. In general, an increase in the size of the metal atom results in an increase in the extent of metal association. For example, titanium has an atomic radius of 1.32 Å and a degree of oligomerization of 2.4. Thallium, on the other hand, has an atomic radius of 1.55 Å and a degree of oligomerization of 6.0.

From a structural point of view, Bradley [87] formulated a theory relating the extent of association of alcoxides to the coordination number of the central metal atom. According to his theory, alcoxides tend to form smaller molecular units when the central atom has a high coordination number. For example, TEOS forms monomers, ATB forms dimers, $Ti(OEt)_4$ forms a mixture of oligomers and LiOBut forms hexamers. From a chemical point of view, the degree of polymerization is a function of the hydrolysis reaction and other experimental variables.

2.1.6. Volatility

This property is directly related to the molecular size, the structure of the alkyl group, and the properties of the central metal atom. These properties will influence the polarity of the M–O–C bond. Intermolecular forces also play a role. In general, large alkyl groups will tend to reduce the alcoxide volatility.

2.1.7. Viscosity

When the extent of polymerization is high, viscosity will increase. In the sol–gel process, the alcoxides are generally dissolved in alcohols. The viscosity will be a function of the concentration of the solute, the solubility of the alcoxide in the solvent and the interaction between the molecules in solution.

2.1.8. Alcoholysis reactions

When the alcoxides are dissolved in alcohols prior to initiating a sol–gel synthesis reaction, it is generally assumed that the solvent is inert. However, this is not necessarily true. The possibility of reactions occurring between the alcoxides and the solvent alcohol molecules may have a significant effect on the synthesis reactions. Two possibilities may exist as follows: in the first case, the alcoxide is dissolved in an alcohol having matching alkyl groups, i.e., TEOS in ethyl alcohol. In the second case, the alcoxide is dissolved in an alcohol which has different alkyl groups. When the alcohol and the alcoxide have identical alkyl groups, the same alcohol is produced as a reaction product and is part of the reaction equilibria. When the alkyl groups are different, alkyl exchange reactions may occur, complicating the synthesis. The exchange reactions are referred to as alcoholysis reactions:

$$M(OR)_n + xR'OH \rightarrow M(OR)_{n-x}(OR')_x + xROH$$

These reactions may be used to good advantage. A greater homogeneity in the original solution may be achieved, hydrolysis reaction rates can be varied and the active metal precursor can be stabilized in different coordination states within the support [94].

2.1.9. Molecular associations

Molecular association is a required first step in the synthesis of mixed metal oxides. Dislich [95] proposes that polynuclear species are readily formed starting from different metal alcoxides.

$$M(OR)_n + M'(OR)_n \rightarrow \{M[M'(OR)_{n-1}](OR)_n\}$$

Reactions between metal alcoxides having different electronegativities can occur when it is possible to expand the coordination sphere and form complexes as suggested by Dislich [95].

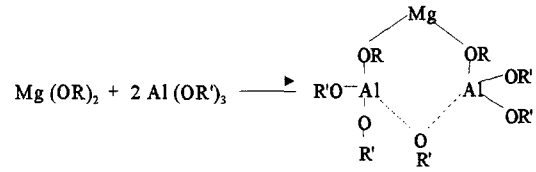

2.1.10. Reactions with organic acids

Organic acids are often used as acid catalysts to hydrolyze the alcoxides. However, they may react with the alcoxides according to the following reaction:

$$M(OR)_n + xRCOOH \rightarrow M(OR)_{n-x}(OOCR)_x + xROH$$

Doeuff et al. [96,97] have shown that the acid first attacks the ligand on the alcoxi groups forming either mono or bidentate ligand. Lopez et al. [98,99] report that the bond formed between the support and the ligand of the organic acid can be broken at relatively low temperatures without contaminating the support. The advantage in the use of organic acids is that one can use several weak organic acids in order to vary the particle size of the support in addition to other physical properties of the support [100,101].

Sulfate promoted metal oxides have recently attracted attention due to their potential use in a variety of catalytic reactions. In particular, the superacid properties of SO_4^{2-}/ZrO_2 have made it attractive in commercial applications related to the upgrading of petroleum feeds with low octane ratings. Because the synthesis of these materials is the subject of another review in this

series [102], we will not dwell on this subject extensively. However, it is important to note that there are two distinctively different methods which are used to synthesize sulfated zirconia by the sol–gel method. A one step synthesis method has been used by Ward and Ko [103]. In this method, the sulfuric acid is added prior to the gelation step. The solvent is removed by supercritical extraction using CO_2. This method results in aerogels which have a mesoporous structure. Pore size distributions are centered between 4.5 and 8.0 nm. Surface areas are approximately 150 m^2/g following calcination at 500°C. Li and Gonzalez [104] have synthesized a series of SO_4^{2-}/ZrO_2 catalysts using a two-step sol–gel approach. The first step involves the synthesis of the gel using $Zr(n\text{-}PrO)_4$ as the precursor and adding water to complete the reaction. Drying at 130°C was used to remove the solvent. The resultant xerogel was pretreated with He at 385°C prior to promotion with sulfuric acid. The concentration of the sulfuric acid was found to be critical. These results are summarized in Table 6.

The activity of these materials in the isomerization of butane parallels the surface area. The most active material corresponds to the catalyst with the largest surface area.

Deactivation rates for the most active catalyst are shown in Fig. 9. In this figure conversions/g of catalysts for both the MEI commercial catalyst and the sol–gel/0.5N H_2SO_4 are shown as a function of time. Conversions are quite comparable. TGA-mass spectrometer studies [104] show that CO_2 is evolved at approximately

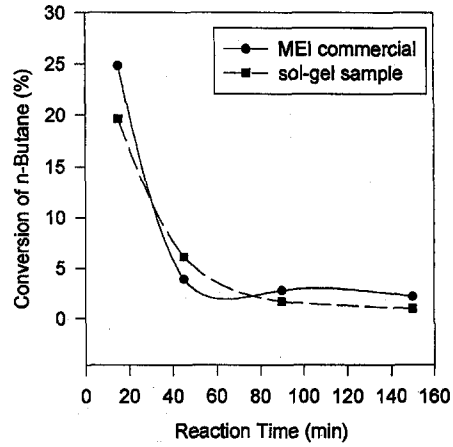

Fig. 9. Comparison of activities of sol–gel and MEI commercial ZrO_2/SO_4^{2-} (carrier gas – N_2) [104].

400°C for the deactivated catalyst. SO_2 loss is observed at approximately 700°C. Activation prior to reaction was at 600°C in O_2 for 1 h. Sulfur was not lost as result of activation at 600°C. The reasons for deactivation are currently a topic of intense debate and will not be discussed any further here.

2.2. Sintering studies of supported metal catalysts

2.2.1. Proposed mechanisms in metal sintering

Catalyst deactivation due to metal sintering has been a serious problem for many years as it shortens the useful life of a catalyst. The overall picture of sintering from experimental observations is that small crystallites diminish in size and larger ones increase. This can be explained by noting that metal–metal bond energies are

Table 6
Physical properties of sulfated zirconia catalysts

Samples	BET (m^2/g)	Pore volume (ml/g)	Average pore diameter (nm)	S (wt%)	Ref.
Sol–gel/0.05N H_2SO_4	112	0.66	3.0	–	[104]
Sol–gel/0.20N H_2SO_4	177	0.33	3.2	1.10	[104]
Sol–gel/0.50N H_2SO_4	186	0.36	3.3	2.48	[104]
Sol–gel/0.75N H_2SO_4	165	0.32	3.2	–	[104]
Sol–gel/1.00N H_2SO_4	106	0.24	3.3	3.96	[104]
Sol–gel/2.00N H_2SO_4	40	0.20	8.0	6.06	[104]
MEI commercial	130	0.15	3.1	1.32	[105]

larger than metal–support interactions. In other words, large crystallites are more stable than small ones. Several mechanisms which deal with the mechanism of sintering have been proposed. However, it is not surprising that sintering is not fully understood. These mechanisms can be grouped into three main types of sintering processes: (a) the emission of single metal atoms [106,107]; (b) crystallite migration via surface diffusion [4,5]; and (c) gas phase or liquid phase transport [2,108]. The predominant mechanism in a typical sintering situation may involve all three depending on sintering temperature, metal precursor, the presence of gaseous reagents which react with the metal to form volatile compounds such as chlorides or oxides, and the extent to which bulk and Knudsen diffusion occurs in a porous medium.

Sintering due to single metal atom emission occurs as the escape of a metal atom from a crystallite, transport of the atom across the surface of the support, and collision with a second metal crystallite. This mechanism is also known as Ostwald ripening or atomic migration. It is reasonable to assume that single metal atom emission from the surface of a metal crystallite may occur at relatively high temperatures when the thermal energy of the metal atoms exceeds the potential well which binds them. It is generally believed that the temperature where this begins to occur for a pure metal is 500–700°C. The concept was initially defined by Chakraverty [106]. The theoretical basis for this mechanism was developed by Flynn and Wanke [107].

A second mechanism involves a crystallite migration model or a Smoluchowski coagulation model. In this mechanism sintering occurs as the result of the migration of the crystallite over the surface of the support. The surface migration of the crystallite might occur under the following conditions: the breaking of bonds between the metal atoms and the substrate (if such bonds exist), a change in the wetting angle between the metal particle and the support, or a change in the interfacial area between a crystallite and the support. The motion of the crystallite over the substrate is the result of the vibration of the particle which is analogous to Brownian motion in two dimensions. The theoretical basis for this model has been developed by Ruckenstein and coworkers [4,5]. An interesting conclusion derived from this model is that when the size of the crystallite is matched to the diameter of the pore, surface diffusion is inhibited and crystal growth will not occur. The surface diffusion coefficient for porous supported metal crystallites is dependent on temperature, surface friction coefficient, and the interfacial area between the crystallite and the support.

$$D_i = 2\kappa T/\mu_i(\Theta_i, \Omega_i)S_i,$$

where D_i is the diffusion coefficient of the crystallite on the substrate, κ is the Boltzmann constant, T is temperature (K), $\mu_i(\Theta_i, \Omega_i)$ is the surface friction coefficient, Θ_i is the wetting angle, Ω_i is the substrate–support interaction, and S_i is the interfacial area between the crystallite and the support. It is important to observe that the substrate could be either a metal or a metal oxide.

In the case of gas phase transport, volatile compounds such as chlorides or oxides are usually involved. The formation of large Ru particles at low oxidation temperature (300–400°C) has been observed on different supports such as alumina [109], Y-zeolite [110], and silica [111]. The substantial Ru loss at relatively low temperatures in oxygen observed by Zou et al. [85] favors the argument for the formation of volatile

Table 7
Changes in metal particle size and pore size distribution as a function of H_2O/TEOS ratios at the same set of conditions: 0.5–0.6% metal loading, O_2, H_2, 400°C pretreatment [114]

H_2O/TEOS	ICP (wt%)	Av. pore size (nm)	Av. particle size (nm)	
			TEM	H-chemisorption
10	0.5	7.5	1.7	1.6
20	0.6	7.0	2.0	1.5
40	0.6	5.0	2.8	2.7
60	0.65	3.5	3.3	2.5

Table 8
Changes in average metal particle size distribution as a function of sintering temperature

Sample	Treatment	BET (m^2/g)	Av. pore size (nm)	Pore volume (ml/g)	Particle size (nm)
IE [a]	O_2, H_2, 400°C	205	24	1.38	1.8
IE	O_2 600°C (24 h), H_2 400°C	198	24	1.37	11.0
Sol–gel	O_2, H_2, 400°C	812	3.5	0.692	3.4
Sol–gel	O_2 675°C (24 h), H_2 400°C	708	3.5	0.526	3.4
Sol–gel	O_2 675°C (48 h), H_2 400°C	605	3.5	0.511	3.6
Sol–gel	O_2 675°C (72 h), H_2 400°C	605	3.5	0.519	3.8

[a] IE: ion-exchanged using $Pt(NH_3)_4(NO_3)_2$ on Cab–O–Sil.

Ru oxides (RuO_4). In this case, the transport process is rapid and net growth rates are controlled by events at the interface. Wynblatt and Gjostein [112] have developed a theory for sintering via diffusion through the vapor phase:

$$(R/R_0)^2 = 1 + \left(K_v/R_o^2\right)^{t/t_0},$$

where R is the average particle radius of the distribution, R_0 is its initial value, K_v is a characteristic rate constant for the interfacial process, and t/t_0 is the time.

In the case of the liquid-phase transport of metal crystallites, the use of the Tamman temperature as a rule of thumb in predicting sintering temperatures is useful. Lyon and Somorjai [108] reported the formation of disordered Pt structures (liquid-like) following heat treatment at the Tamman temperature of Pt. The Tamman

Table 9
Changes in average palladium metal particle size as a function of sintering temperature and atmosphere [a]

Sample	Treatment	BET (m^2/g)	Av. pore diam. (nm)	Pore vol. (ml/g)	D_H (%)	Particle size (nm)	
						TEM	H-Chem
IE-1 (fresh) [b]	He 400°C (1 h)	200	24.0	1.40	94	1.5	1.2
IE-1 (reduced)	O_2 650°C (22 h)	198	24.0	1.37	70		1.6
IE-1 (reduced)	H_2 650°C (22 h)	195	24.0	1.36	43		2.6
IE-2 (fresh) [b]	O_2 300°C (1 h)	204	24.0	1.39	51	2.5	2.2
IE-2 (reduced)	O_2 650°C (22 h)	197	24.0	1.37	43		2.6
IE-2 (reduced)	H_2 650°C (22 h)	196	24.0	1.36	26		4.3
SG-1 (fresh) [c]	O_2 400°C (1 h)	702	3.5	0.37	47	3.0	2.4
SG-1 (reduced)	O_2 650°C (22 h)	651	3.5	0.32	47		2.4
SG-1 (reduced)	H_2 650°C (22 h)	667	3.5	0.33	25		4.5
SG-2 (fresh) [d]	O_2 400°C (1 h)	648	4.0	0.56	20	6.0	5.5
SG-2 (reduced)	O_2 650°C (22 h)	529	4.0	0.51	16		6.9
SG-2 (reduced)	O_2 650°C (70 h)	530	4.0	0.50	16		6.9
SG-2 (reduced)	H_2 650°C (22 h)	541	4.0	0.51	8		13.8
SG-3 (fresh) [e]	O_2 400°C (1 h)	623	3.6	0.62	16	8.0	7.2
SG-3 (reduced)	O_2 650°C (22 h)	557	3.6	0.54	16		7.2
SG-3 (reduced) [f]	H_2 650°C (22 h)	584	3.6	0.56	8		13.6

[a] Prior to ICP, chemisorption and TEM measurements, all samples were reduced in H_2 at 400°C for 1 h following sintering.
[b] IE-1: ion-exchanged sample with an ICP metal loading of 1.55 wt%.
[c] SG-1: sol–gel sample with a H_2O/TEOS ratio of 10, pH 4.60, gelation temperature 50°C (18 h), 80°C (1 h), ICP 0.80 wt% metal loading.
[d] SG-2: xerogel sample with a H_2O/TEOS ratio of 17.5, pH 3.69, gelation temperature 75°C (2 h), ICP 0.92 wt% metal loading.
[e] SG-3: xerogel sample with a H_2O/TEOS ratio of 15, pH 3.71, gelation temperature 75°C (2 h), ICP 1.25 wt% metal loading.
[f] ICP 1.24 wt% metal loading obtained following sintering SG-3 in H_2 at 650°C (22 h).

temperature ($T_m/2$) of Pt is 750°C. Ducros and Merrill [113] observed the formation of an elongated LEED pattern following pretreatment in oxygen at 800°C.

2.2.2. The synthesis of thermally stable catalysts by the sol–gel method

Zou and Gonzalez [114] successfully achieved an excellent match between average pore size distribution and metal particle size. In these studies $Pt(AcAc)_2$ was used as the metal precursor and the H_2O/TEOS ratio was varied. The data obtained in this study is summarized in Table 7.

This data suggests that a H_2O/TEOS ratio of 60 should be optimum. Sintering studies were carried out and this data is shown in Table 8. Catalysts prepared by traditional methods are included for comparison purposes.

Zou and Gonzalez [36] were also successful in synthesizing Pd/SiO_2 catalysts with high tolerance to thermal treatment. These studies are summarized in Table 9.

It is apparent from this data that Pd is stable to sintering in an O_2 atmosphere. Under these conditions, the surface species which is diffusing is undoubtedly PdO which forms readily at about 350°C. Decomposition of PdO occurs above 800°C. The thermal stability of supported Pd in a H_2 atmosphere is rather poor. Although the formation and splitting of Pd–β-hydride on alumina has been reported [25,28,29], the formation of this hydride phase is questionable at high temperatures. A more likely reason for this thermal instability is the high solubility of H_2 in Pd which may result in the weakening of Pd–Pd bonds. Perhaps bimetallic clusters in which Pd is alloyed with a second metal may inhibit this H_2 solubility and result in materials with higher thermal stability.

3. Catalytic properties

To be useful, supported metal catalysts prepared by the sol–gel method should have catalytic activities and selectivities which are comparable to catalysts prepared by more traditional methods. In addition to the desirable thermal properties, they should also resist deactivation and show high mechanical stability. In other words, carbon deposition leading to pore mouth poisoning and the breakdown of the large porous network following thermal treatment would lead to materials which would be unacceptable. For this reason, comparisons with supported metal catalysts prepared by traditional methods need to be made. In this final section we will summarize data obtained on Pt/SiO_2, Pt/Al_2O_3, and $Pt–Sn/Al_2O_3$ in order to support our view that catalysts prepared by the sol–gel method are competitive with catalysts prepared by both im-

Table 10
Changes in the physicochemical properties of Pt/SiO_2 catalysts before and after deactivation under reaction conditions: 400°C, H_2–n-hexane molar ratio of 17

Catalyst	wt%	BET (m^2/g)	Pore diam. (nm)	Pore vol. (ml/g)	D_H (%)	TOF × 10^3 molec site^{-1} s^{-1}	Ref.
Xerogel [a]	0.8	729	7.0	0.78	75	65	[44]
Xerogel [b]		690	7.0	0.72	68	45	[44]
Ion-ex [a]	0.65	205	24	1.38	80	48	[44]
Ion-ex [b]		193	24	1.31	70	30	[44]
81 Ion XS [a,c]	0.83	295	14	1.30	75	53	[116]
81 Ion XS [b]		284	14	1.27	55	36	[116]
Impreg. [a]	0.91	754	11	2.62	15	38	[44]
Impreg. [b]		786	11	2.61	12		[24]

[a] Fresh catalysts after standard pretreatment in O_2 at 400°C for 1 h and H_2 at 400°C for 6–8 h.
[b] Deactivated catalysts following reaction in H_2/n-hexane at 400°C for 6–8 h.
[c] Samples from J.B. Butt's group at Northwestern University [116].

Table 11
First order deactivation rate constants based on the disappearance of n-hexane

Catalysts	Particle size (nm)	Deactivation rate constant $k_d \times 10^3$ (h^{-1}) at 400°C	Ref.
Ion-exchange	1.5	218	[44]
Xerogel	1.7	221	[44]
Impregnation	6.0	265	[44]
Aerogel	10.5	328	[44]

pregnation and ion-exchange methods. In addition, they also have a much higher degree of thermal resistance. Because most of the catalytic data was obtained using the reforming reactions of n-hexane [44,50,115], we will focus on comparative reaction studies based on this reaction.

3.1. The n-hexane reaction on Pt/SiO_2

Initial reaction rates based on the conversion of n-hexane are summarized in Table 10. Turnover frequencies were comparable for all of the catalysts tested. First order deactivation rates for these catalysts are shown in Table 11.

These data show that silica supported metal xerogels perform as well as or perhaps a little better than supported metal catalysts prepared by other methods. Deactivation rate constants calculated according to the method outlined by Levenspiel [117] appear to be more dependent on particle size that on method of preparation. This is, in part, due to the demanding nature of coke formation which is favored on large particles. However, a major advantage of high-surface-area materials is that metal interparticle distances are large and coke can be accommodated more easily on this larger surface area.

Selectivity studies based on eleven products grouped together as hydrogenolysis, isomerization, or cyclization reactions were performed. These studies also showed little difference with regard to method of preparation. Selectivity differences appear to be more related to differences in dispersion.

A very important feature of these studies is that the metal particles are not occluded as one might expect. TEM, H_2 chemisorption and CO chemisorption measurements were invariably in good agreement [44]. The open porous structure of these materials allows easy access of the reactants to the surface of the metal. Moreover, this access is not significantly affected by catalyst deactivation.

3.2. The n-hexane reaction on Pt/Al_2O_3 xerogels

All Pt-containing alumina xerogels studied are active [50] in the reforming reactions of n-hexane. Within experimental error, differences in selectivity between hydrogenolysis (~ 20%), isomerization (~ 45%) and dehydrocyclization (~ 35%) were small. Reaction rate measurements obtained at 325°C after 0.5 h on stream are summarized in Table 12.

It is important to note that the data in Table 12 is arranged in order of increasing pore diameters. Changes in the average pore diameter

Table 12
Turnover frequencies for the reactions of n-hexane at 325°C after 0.5 h on stream [50]

Catalyst	Dispersion (%)	Conversion (%)	Pore diam. (nm)	TOF $\times 10^3$ (s^{-1})	Ref.
1.0 Pt/90% Al_2O_3–10% SiO_2	58	6.7	4	23.1	[50]
1.0 Pt/Al_2O_3 (xerogel)	53	8.4	5	26.5	[50]
1.0 Pt/Al_2O_3 (xerogel)	74	10.8	9	28.6	[50]
1.0 Pt/Al_2O_3 (xerogel)	61	14.7	15	36.6	[50]
1.0 Pt/Al_2O_3 (aerogel)	40	11.4	19	44.4	[50]

were accomplished by varying the H_2O/alcoxide ratio during synthesis.

The size of the pores in the samples does seem to have an effect on the conversion of n-hexane as determined from the variations in turnover frequencies. It is clear that there is an increasing trend noticeable in the TOF values as the average pore diameter is increased. The largest TOF was obtained in the case of the 1.0 Pt/alumina aerogel sample that had the largest average pore diameter. It is important to observe that this TOF dependence is not observed for Pt/SiO_2 xerogel samples. It must be remembered that the n-hexane–H_2 reaction over Pt/Al_2O_3 is bifunctional whereas over Pt/SiO_2, the reaction occurs only on the metal surface. The mixed metal oxide sample which has the smallest average pore diameter also shows the lowest TOF value. The values for the three 1.0 Pt/Al_2O_3 xerogels lie in between the values obtained for the xerogel and the mixed metal oxide sample. The advantage of having large pores could be that pore blocking by carbonaceous deposits is less likely to occur in larger pores as compared to smaller pores during the reactions of n-hexane.

First-order deactivation rate constants determined by the method outlined by Levenspeil [117] are shown in Table 13 [50].

This data shows that there is a correlation between the BET surface area of the sample and the k_d value. A decrease in the BET surface area results in a greater rate of deactivation because there is less surface area to accommodate carbonaceous residues. Under these conditions, the Pt sites are more easily poisoned. A higher BET surface area appears to be beneficial for activity maintenance.

These observations show the versatility of the sol–gel method. A careful control of the conditions under which the synthesis is carried out, enables one to control the physical and catalytic properties of the resulting catalyst.

Table 13
First-order deactivation rate constants for the reactions of n-hexane at 400°C

Catalyst	Conversion (%)	BET area (m^2/g)	k_d (h^{-1})	Ref.
1.0 Pt/90% Al_2O_3–10% SiO_2	22.9	512	0.255	[50]
1.0 Pt/Al_2O_3 (xerogel)	37.9	490	0.256	[50]
1.0 Pt/Al_2O_3 (xerogel)	46.9	363	0.264	[50]
1.0 Pt/Al_2O_3 (aerogel)	41.0	306	0.301	[50]
1.0 Pt/Al_2O_3 (xerogel)	30.3	222	0.329	[50]

3.3. The n-butane reaction on $Pt–Sn/Al_2O_3$

Alumina-supported Pt–Sn catalysts are industrially important because of their potential for use in naphtha reforming. These catalysts are especially promising for low-pressure operation and in processes in which continuous regeneration is performed [118]. An important characteristic of these bimetallic catalysts is that they display higher stability during reaction compared to monometallic Pt catalysts. The reason for this improved stability is believed to be due to a change in the catalytic selectivity that leads to a suppression of coke-forming reactions in comparison with reforming reactions [119]. $Pt–Sn/Al_2O_3$ catalysts have been traditionally prepared by impregnation methods. For this reason it is of interest to explore improvements which may come about using sol–gel processing.

The physical properties of $Pt–Sn/Al_2O_3$ bimetallic catalysts prepared using $H_2PtCl_6 \cdot xH_2O$, $SnCl_4 \cdot 5H_2O$ and ATB are shown in Table 14.

This data suggests a gradual increase in the coverage of Pt by Sn with increasing Sn loading. The catalytic selectivity at constant n-hexane conversion for this series of $Pt–Sn/Al_2O_3$ catalysts is shown in Table 15.

In an observation similar to this, a very high isomerization selectivity was observed for a catalyst having a high Sn loading [120]. It was also found that in the case of traditionally prepared samples, there was an increase in the isomerization selectivity and a decrease in the hy-

Table 14
Physical properties of $Pt–Sn/Al_2O_3$ catalysts

Catalyst	BET area (m^2/g)	Pore volume (ml/g)	Av. pore diam. (nm)	H/Pt	Ref.
Blank Al_2O_3	503	1.89	5.8		[115]
1.0 Sn/Al_2O_3	541	2.03	5.8		[115]
1.0 Pt/Al_2O_3	461	1.99	5.9	0.70	[115]
1.0 $Pt–0.3Sn/Al_2O_3$	453	1.84	5.9	0.57	[115]
1.0 $Pt–0.9Sn/Al_2O_3$	434	2.01	5.9	0.30	[115]
1.0 $Pt–1.5Sn/Al_2O_3$	455	2.21	4.8	0.21	[115]

drogenolysis selectivity with increasing amounts of Sn in the sample. However, there is one important difference between the study on traditionally prepared catalysts and catalysts prepared by the sol–gel method. In the case of traditionally prepared samples it was found that when the designed Pt loading was kept constant at 1 wt% and the amount of Sn was increased gradually, then for small amounts of tin addition (up to a designed loading of 0.5 wt%) the isomerization selectivity did not increase by a very large amount [120]. When the designed loading of tin was increased beyond 0.5 wt% to 1.0 wt%, there was a large increase in the isomerization selectivity, from 39.6% to 95.5% [120]. On the other hand, in the case of the sol–gel samples a more gradual increase in the isomerization selectivity was observed. A possible reason for this could be that in the case of the traditionally prepared samples, at low loadings of Sn, the Pt and Sn are segregated and hence the isomerization selectivity does not change very much. On the other hand, in the sol–gel samples the Sn and Pt interact more strongly at lower Sn loadings and hence the effect on the isomerization selectivity is more gradual.

4. Conclusions and recommendations for future studies

Potential applications of catalysts prepared by sol–gel processing are tied to their high thermal stability, their resistance to deactivation and the flexibility that one has in the control of physical properties such as porosity, surface area and pore diameter.

In the synthesis of supported metal catalysts, major emphasis has been placed on techniques which yield high metal dispersions and thermally resistant catalysts. To a large extent these properties can be controlled by maximizing support–metal precursor interactions, BET surface areas and support pore structure. The methods of choice over the past thirty years have been ion-exchange and impregnation. Although these methods, when carefully used, yield highly dispersed, active catalysts, the versatility of sol–gel techniques add a flexibility dimension not pre-

Table 15
Catalytic selectivity over a series of $Pt–Sn/Al_2O_3$ catalysts at a total n-hexane conversion of approximately 10%

Catalysts	T (°C)	Conversion (%)	Selectivity (%)			Ref.
			Dehydrocyclization	Isomerization	Hydrogenation	
1.0 Pt/Al_2O_3	300	12.2	6.3	46.2	47.5	[115]
1.0 $Pt–0.3Sn/Al_2O_3$	333	11.4	7.6	62.7	29.7	[115]
1.0 $Pt–0.9Sn/Al_2O_3$	355	9.1	2.4	95.2	2.4	[115]
1.0 $Pt–1.5Sn/al_2O_3$	390	12.6	2.0	96.3	1.7	[115]

sent with the traditional preparative techniques. The sol–gel method enables the researcher to explore the use of supports other than silica and alumina and to prepare mixed oxide supports by well-defined synthesis routes.

A wide variety of supported metal catalysts prepared by both impregnation and ion-exchange methods have been used in commercial applications. Spherical pellets, extrudates and a variety of other types of supports can be impregnated with metal precursors and used as catalytic materials. In recent years, a great deal of emphasis has been placed on the synthesis of ceramic monolithic materials and catalytic membranes used as support materials for automotive catalytic converters and other catalytic applications. In order to use a ceramic monolith in a catalytic application, it is necessary to coat it with the active catalytic phase. This is usually a two step process. The first step in the process involves coating the ceramic monolith with a support phase such as silica or alumina. Following thermal treatment to convert the gel into the desired active phase, the second step in the process involves the use of a metallic precursor to deposit the active metallic phase.

In the current review, using several examples, we have attempted to show that it might be possible to reduce the number of steps in preparing supported metal coatings on monoliths. Using sol–gel processing technology, metal precursors can be stabilized on the support in the form of a sol, and coating of the monolith can be accomplished in a single step. The properties of the supported metal catalysts are comparable and in some cases superior to catalysts prepared using conventional methods of preparation.

Catalytic coatings of membranes and monoliths have aroused much interest in the design of tubular reactors. The diffusion of reactants and products in these systems is generally limited to a few μm. For this reason, catalytic materials prepared by sol–gel methods having controlled porosity are of considerable promise in the development of these devices. Diffusional studies through porous membranes and ceramic materials have become an important area of research within the reaction engineering community.

Results to date in such reactions as hydrogenation, isomerization, oxidation, and catalytic reforming have encouraged us to be optimistic regarding the future of sol–gel processing in the synthesis of catalytic materials which have potential use as coatings for membranes and monoliths.

Future research in the development and modification of support properties is and area in which sol–gel processing may help play an important role. The addition of dopants such as silica, alumina, magnesia, titania, chromia, or zirconia, and the synthesis of mixed oxides are ideally suited to sol–gel processing. Of major significance is the possibility of phase stabilization through the addition of a second oxide. For example, the addition of H_2PtCl_6 to titania during the gel stage results in the stabilization of the anatase phase of titania at a temperature which is considerably higher than that at which a phase change to rutile is normally observed [125].

The synthesis of highly dispersed inexpensive transition metals such as Cu, Fe, and Co using sol–gel processing is of interest. Many of these catalysts may be of use in important industrial reactions such as NO_x reduction. In general, highly dispersed Fe, Co, and Cu catalysts are difficult to synthesize using traditional methods.

In conclusion, we would encourage further research in the area of sol–gel processing, with a focus on their potential application as catalysts.

Acknowledgements

Financial support from the U.S. Department of Energy (Basic Energy Science DOE FG02-86ER-1351), The Petroleum Research fund of the American Chemical Society (ACS-PRF #26247-ACS) and The National Science Foun-

dation through a cooperative international grant with Mexico is gratefully acknowledged.

References

[1] S.A. Stevenson, J.A. Dumesic, R.T.K. Baker and E. Ruckenstein (Eds.), Metal Support Interactions in Catalysis, Sintering and Redispersion, Van Nostrand–Reinhold, New York, 1987, pp. 141–303.
[2] M. Chen and L.D. Schmidt, J. Catal., 55 (1978) 348.
[3] T.A. Dorling, B.W.J. Lynch and R.L. Moss, J. Catal., 20 (1971) 190.
[4] E. Ruckenstein and B. Pulvermacher, J. Catal., 29 (1973) 224.
[5] E. Ruckenstein and B. Pulvermacher, J. Catal., 37 (1975) 416.
[6] G.B. McVicker, R.L. Garten and R.T.K. Baker, 5th Canadian Symp. of Catalysis, (1977) p. 346.
[7] Y.C. Pan and G. Ciprious, Rep. EPRI-EM-883 (1978).
[8] A. Thayer, Chem. Eng. News, March 8 (1993) 6.
[9] Chem. Eng. News, March 7 (1994) 9.
[10] Y.L. Lam and M. Boudart, J. Catal., 47 (1977) 393.
[11] M. Chen and L.D. Schmidt, J. Catal., 56 (1979) 198.
[12] W. Zou, Ph.D. Thesis, Tulane University, New Orleans, LA, 1994.
[13] J.J. Chen and E. Ruckenstein, J. Phys. Chem., 85 (1981) 1606.
[14] J.H. Norman, H.G. Staley and E.B. Wayne, J. Phys. Chem., 69 (1965) 1373.
[15] G.I. Goncharenko, V.B. Lazarev and I.S. Shaplygin, Russ. J. Inorg. Chem., 30 (1985) 1723.
[16] S.E. Wanke, J.A. Szymura and T.T. Yu, in E.E. Petersen and A.T. Bell (Eds.), Proc. Int. Symp. Catal. Deact., Marcel Dekker, New York, 1986, p. 65.
[17] R.M.J. Fiederow, B.S. Chahar and S.E. Wanke, J. Catal., 51 (1978) 193.
[18] R.J. Farrauto, R.M. Heck and B.K. Speronello, Chem. Eng. News, 7 Sept. (1992) 34.
[19] R.L. Klimisch, J.C. Summers and J.C. Schlatter, in J.E. McEvoy (Ed.), Catalysis for the Control of Automotive Pollutants, Advances in Chemistry Series No. 143, ACS, Washington, D.C., 1975.
[20] P.C. Aken, J. Catal., 10 (1968) 224.
[21] R. Lamber, N. Jaeger and G. Schulz-Ekloff, in C. Morterra, A. Zecchina and G. Costa (Eds.), Structure and Reactivity of Surface, Elsevier, Amsterdam, Netherlands, 1989, pp. 559–565.
[22] W. Juszczyk. Z. Karpinski, J. Pielaszek, I. Ratajczkowa and Z. Stanasiuk, in M.J. Phillips and M. Ternan (Eds.), Proc. 9th Int. Congress on Catalysis, Calgary, Canada, 1988, p. 1238.
[23] O. Leonte, M. Birjega, N. Popescu-Pogrion, C. Sarbu, D. Marcovei, P. Pausescu and M. Georgescu, Proc. 8th Int. Congress on Catalysis Vol. II, Dechenow, Frankfort, 1984, p. 683.
[24] D.H. Everett and P.A. Sermon, J. Phys. Chem., 114 (1979) 109.
[25] R. Golub and D.B. Dadyburjor, J. Catal., 68 (1981) 473.
[26] R.K. Nandi, P. Pitchai, S.S. Wong, J.B. Cohen, R.L. Burwell Jr. and J.B. Butt, J. Catal., 70 (1981) 298.
[27] M. Boudart and H.S. Wang, J. Catal., 39 (1975) 44.
[28] J.J. Chen and E. Ruckenstein, J. Catal., 69 (1981) 254.
[29] M. Hino and K. Arata, Chem. Lett., (1979) 1259.
[30] K. Tanabe, in B.L. Shapiro (Ed.), Heterogeneous Catalysis, Texas A&M Univ. Press, 1984, p. 71.
[31] M. Hino and K. Arata, Chem. Lett., (1980) 963.
[32] K. Arata and M. Hino, Bull. Chem. Soc. Jpn., 44 (1980) 385.
[33] M. Hino and K. Arata, Chem. Lett., (1979) 1259.
[34] S. Baba, Y. Shibata, H. Tkaoka, T. Kimura and K. Takasaka, Japan Patent 61-153140 (1986).
[35] V.T. Zaspalis, W. Van Praag, K. Keizer, J.G. Van Owmen, J.R.H. Ross and A. Burgraaf, J. Appl. Catal., 74 (1991) 223.
[36] W. Zou and R.D. Gonzalez, Appl. Catal. A, 126 (1995) 351.
[37] A.J. Burggraaf and K. Keizer, in R.R. Bhave (Ed.), Inorganic Membranes: Synthesis, Characteristics and Applications, Van Nordstrand–Reinhold, New York, 1991, p. 10.
[38] S.J. Teichner, in J. Frick (Ed.), Aerogel, Springer, Berlin, 1986, p. 22.
[39] O.V. Krylob, Catalysis by Nonmetals, Academic Press, New York, 1970.
[40] W. Zou and R.D. Gonzalez, Catal. Lett., 12 (1992) 73.
[41] A.L. Bonivardi and M.A. Baltanas, J. Catal. 125 (1990) 243.
[42] M. Viniegra, R. Gomez and R.D. Gonzalez, J. Catal. 111 (1988) 429.
[43] B. Samanos, P. Boutry and R.C.R. Montarnal, Acad. Sci. Ser. C, 274 (1972) 575.
[44] W. Zou and R.D. Gonzalez, J. Catal., 152 (1995) 291.
[45] L.C. Klein, Ann. Rev. Mar. Sci., 15 (1985) 227.
[46] B.E. Yoldas, J. Sol–Gel Sci. Tech., 1 (1993) 65.
[47] T. Lopez, M. Asomoza, L. Razo and R. Gomez, J. Non-Cryst. Solids, 108 (1989) 45.
[48] L.K. Campbell, B.K. Na and E.I. Ko, Chem. Mater., 4 (1992) 1329.
[49] S.J. Teichner, G.A. Nicolaon, M.A. Vicarini and G.E.E. Gardes, Adv. Colloid Interface Sci., 5 (1976) 245.
[50] K. Balakrishnan and R.D. Gonzalez, J. Catal., 144 (1993) 395.
[51] T. Lopez, P. Bosch, M. Moran and R. Gomez, J. Phys. Chem., 97 (1993) 1671.
[52] T. Lopez, L. Herrara, J. Mendez, P. Bosch, R. Gomez and R.D. Gonzalez, J. Non-Cryst. Solids, 147 (1992) 753.
[53] C. Sanchez and J. Livage, New J. Chem., 14 (1990) 513.
[54] T. Lopez, M. Asomoza, P. Bosch, E. Garcia-Figueroa and R. Gomez, J. Catal., 138 (1992) 463.
[55] H. Schmidt, J. Non-Cryst. Solids, 112 (1989) 419.
[56] K. Tanabe, Mater. Chem. Phys., 13 (1985) 347.
[57] H.D. Gesser and P.C. Goswami, Chem. Rev., 89 (1985) 765.
[58] K.J. McNeil, J.A. Dicarpio, D.A. Walsh and R.F. Pratt, J. ACS, 102 (1980) 1859.
[59] E.J.A. Pope and J.D. Mackenzie, J. Non-Cryst. Solids, 87 (1986) 185.

[60] C.L. Rollinson, in J.C. Ballar (Ed.), The Chemistry of the Coordination Compounds, Rheinhold, New York, 1956.
[61] M. Ardon and B. Magyar, J. ACS, 106 (1984) 3359.
[62] V. Baran, Coord. Chem. Rev., 6 (1971) 65.
[63] C.J. Brinker and G.W. Sherer, Sol–Gel Science, Academic Press, San Diego, 1990.
[64] C.M. Pajonk, Appl. Catal., 72 (1991) 217.
[65] G.A. Nicolaon and S.J. Teichner, Bull. Soc. Chim. Fr., 8 (1968) 3107.
[66] C.G. Swain, R.M. Esteve and R.H. Jones, J. ACS, 71 (1949) 965.
[67] M. Yamane, S. Aso, S. Okano and T. Sakaino, J. Mater. Sci., 14 (1979) 607.
[68] R.K. Iler, The Chemistry of Silica, Wiley, New York, 1970.
[69] T. Lopez, React. Kinet. Catal. Lett., 47 (1992) 21.
[70] T. Lopez, M. Asomoza and R. Gomez, J. Non-Cryst. Solids, 147 (1992) 769.
[71] C. Sanchez and J. Livage, New J. Chem., 14 (1990) 513.
[72] A. Boonstra and T. Benards, J. Non-Cryst. Solids, 105 (1988) 207.
[73] K.A. Andrianov, Metal Organic Polymers, Wiley, New York, 1965.
[74] R. Aelion, A. Loebel and F. Eirich, J. ACS, 72 (1950) 5705.
[75] C.G. Swain, R.M. Esteve and R.H. Jones, J. ACS, 71 (1949) 965.
[76] E.J.A. Pope and J.D. Mackenzie, J. Non-Cryst. Solids, 87 (1986) 185.
[77] K.S.W. Sing, D.H. Everett, R.A.W. Haul, L. Moscou, R.A. Pieroti, J. Roqueral and T. Siemieniewska, Pure Appl. Chem., 57 (1985) 603.
[78] T. Lopez, I. Garcia and R. Gomez, J. Catal., 127 (1991) 75.
[79] T. Lopez, I. Garcia and R. Gomez, Mater. Chem. Phys., 36 (1993) 222.
[80] C.J. Brinker and G.W. Sherer, J. Am. Ceram. Soc., 69 (1986) 12.
[81] C.J. Brinker, E.P. Roth, G.W. Sherer and D.R. Tallant, J. Non-Cryst. Solids, 71 (1985) 171.
[82] C.J. Brinker, E.P. Roth, D.R. Tallant and G.W. Scherer, in L.L. Hench and D.R. Ulrich (Eds.), Science of Ceramic Chemical Processing, Wiley, New York, 1986, p. 137.
[83] T. Lopez, A. Romero and R. Gomez, J. Non-Cryst. Solids, 127 (1991) 307.
[84] J.N. Armor, E.J. Carlson and P.M. Zambri, Appl. Catal., 19 (1985) 339.
[85] T. Lopez, L. Herrara, R. Gomez, W. Zou, K. Robinson and R.D. Gonzalez, J. Catal., 136 (1992) 621.
[86] D.C. Bradley, Metal Alkoxides and Dialkylamides, Adv. in Inorg. Chem. and Radiochem. Vol 15, Academic Press, 1972.
[87] D.C. Bradley, Nature, 182 (1958) 1211.
[88] E.M. Rabinovich, J. Mater. Sci., 20 (1985) 4259.
[89] D.C. Bradley, R.C. Mehnotra and D.P. Gaur, Metal Alcoxides, Academic Press, New York, 1978.
[90] S. Sakka and K. Kamiya, J. Non-Cryst. Solids, 42 (1980) 403.
[91] G.W. Sherer and Yogyo-Kyokai-Shi, J. Non-Cryst. Solids, 95 (1987) 21.
[92] S. Sakka, Am. Ceram. Soc. Bull., 63 (1984) 1136.
[93] G. Phillip and H. Schmidt, J. Non-Cryst. Solids, 63 (1984) 283.
[94] T. Lopez, J. Navarette, R. Gomez, O. Novaro, H. Armendaris and F. Figueras, Appl. Catal. A, 125 (1995) 217.
[95] H. Dislich, Angew. Chem. Int. Ed. Engl., 10 (1971) 363.
[96] S. Doeuff, M. Henry, C. Sanchez and J. Livage, J. Non-Cryst. Solids, 89 (1987) 84.
[97] S. Doeuff, M. Henry, C. Sanchez and J. Livage, J. Non-Cryst. Solids, 89 (1987) 206.
[98] T. Lopez and E. Sanchez, React. Kinet. Catal. Lett., 48 (1992) 295.
[99] T. Lopez, E. Sanchez, P. Bosch, Y. Meas and R. Gomez, Mater. Chem. Phys., 32 (1992) 141.
[100] T. Lopez, I. Garcia and R. Gomez, J. Catal., 127 (1991) 75.
[101] D.R. Acosta, O. Novaro, T. Lopez and R. Gomez, J. Mater. Res., 10 (1995) 1.
[102] E. Ko et al., submitted for publication.
[103] D.A. Ward and E.I. Ko, Chem. Mater., 5 (1993) 956.
[104] B. Li and R.D. Gonzalez, Ind. Eng. Chem. Res., 35 (1996) 3141.
[105] P. Moles, reprinted from Specialty Chem., (Nov/Dec 1992).
[106] B.K. Chakraverty, Phys. Chem. Solids, 28 (1967) 2401.
[107] P.C. Flynn and S.E. Wanke, J. Catal., 34 (1974) 390, 400.
[108] H.B. Lyon and G.A. Somojai, J. Chem. Phys., 46 (1967) 2539.
[109] Z.Z. Lin, T. Okuhara and M. Misono, J. Phys. Chem., 92 (1988) 723.
[110] J.R. Pearce, B.L. Gustafson and J.H. Lunsford, Inorg. Chem., 20 (1981) 2957.
[111] S. Alerasool and R.D. Gonzalez, J. Catal., 124 (1990) 204.
[112] P. Wynblatt and N.A. Gjostein, Prog. Solid State Chem., 9 (1975) 1.
[113] R. Ducros and R.P. Merrill, Surf. Sci., 55 (1976) 227.
[114] W. Zou and R.D. Gonzalez, Appl. Catal., 102 (1993) 181.
[115] K. Balakrishnan and R.D. Gonzalez, Langmuir, 10 (1994) 2489.
[116] J. Butt, personal communication.
[117] O. Levenspiel, Chemical Reaction Engineering, Wiley, New York, 1972, pp. 537–551.
[118] R. Srinivasan, L.A. Rice and B.H. Davis, J. Catal., 129 (1991) 257.
[119] R. Burch, J. Catal., 71 (1981) 348.
[120] A. Sachdev, Ph.D. Thesis, University of Michigan, Ann Arbor, Michigan, 1989.
[121] T. Lopez, J. Mendez, R. Gomez and A. Campero, Latin Am. Appl. Res., 6 (1990) 167.
[122] T. Lopez, A. Romero, A. Chavela, L. Razo and R. Gomez, React. Kinet. Catal. Lett., 43 (1991) 461.
[123] T. Lopez, J. Naverrete, R.D. Gonzalez and R. Gomez, J. Mater. Synth. Proc., 2 (1994) 305.
[124] T. Lopez, R. Gomez, E. Romero and I. Schifter, React. Kinet. Catal. Lett., 49 (1993) 95.
[125] T. Lopez and R. Gomez, in L.C. Klein (Ed.), Sol–gel Optics: Processing and Applications, Kluwer, Boston, 1994, Ch. 16, p. 345.